IOP Publishing | International Atomic Energy Agency Nuclear Fusion

Nucl. Fusion **57** (2017) 114001 (6pp) https://doi.org/10.1088/1741-4326/aa7d14

Letter

Excitation of low frequency Alfven eigenmodes in toroidal plasmas

Yaqi Liu[1,2], Zhihong Lin[2,a], Huasen Zhang[1] and Wenlu Zhang[2,3]

[1] Fusion Simulation Center, Peking University, Beijing 100871, People's Republic of China
[2] Department of Physics and Astronomy, University of California, Irvine, CA 92697, United States of America
[3] Institute of Physics, Chinese Academy of Science, Beijing 100190, People's Republic of China

E-mail: zhihongl@uci.edu

Received 18 April 2017, revised 4 June 2017
Accepted for publication 3 July 2017
Published 28 July 2017

Abstract

Global gyrokinetic simulations find that realistic density gradients of energetic particles can simultaneously excite low frequency Alfven eigenmodes in toroidal geometry, beta-induced Alfven-acoustic eigenmode (BAAE) and beta-induced Alfven eigenmode (BAE), with similar radial mode widths and comparable linear growth rates even though damping rate of BAAE is much larger than BAE in the absence of energetic particles. This surprising result is attributed to non-perturbative effects of energetic particles that modify ideal BAAE mode polarizations and nonlocal geometry effects that invalidate radially local dispersion relation. Dominant mode changes from BAAE in a larger tokamak to BAE in a smaller tokamak due to the dependence of wave-particle resonance condition on the tokamak size.

Keywords: energetic particle, acoustic wave, shear Alfvén wave

(Some figures may appear in colour only in the online journal)

The interaction between energetic particles and Alfven waves is an important physical process in laboratory, space, and astrophysical plasmas [1, 2]. In particular, low frequency Alfven eigenmodes in toroidal geometry, such as beta-induced Alfven-acoustic eigenmode (BAAE) [3] and beta-induced Alfven eigenmode (BAE) [4–7], can cause significant loss of energetic particles in fusion plasmas [8]. These discrete frequency modes are a major concern for current fusion experiments that rely on plasma heating by neutral beam injection and future burning plasmas that require self-heating by energetic fusion products (α-particles). BAAE-like fluctuations with a frequency below geodesic acoustic frequency [9] have been observed in DIII-D [10], JET [3, 11], NSTX [12] and ASDEX [13] tokamaks, and LHD [14], HSX [15], and H-1 [16] stellarators. Since BAAE has strong interactions with both thermal and energetic particles due to its low frequency, it can be excited by either energetic [3] or thermal particles [10, 17], and may affect thermal plasma transport. It might also serve as a channel for directly converting kinetic energy of α-particles to thermal ion energy [18], a potentially favorable operating scenario for burning plasmas experiment ITER (ITER webpage). Therefore, it is important to understand the BAAE excitation mechanism and nonlinear dynamics, and the extrapolation from current tokamaks to ITER.

The BAAE was first suggested by an ideal magnetohydrodynamic (MHD) local theory [3], which only predicts a low frequency BAAE gap generated by toroidal coupling of shear Alfven continuum and ion acoustic continuum. However, the existence of discrete frequency BAAE has never been predicted by analytic theory, although discrete frequency modes inside the low frequency gap have been found by ideal MHD eigenvalue codes such as NOVA [3, 11]. This ideal MHD eigenmode of thermal plasmas can then be used to calculate wave-particle energy exchanges for BAAE excitation by pressure gradients of energetic particles, an approach known as perturbative theory [10]. However, a gyrokinetic theory [19]

[a] Author to whom any correspondence should be addressed.

argued that strong Landau damping by thermal ions would prevent a significant response to acoustic polarizations in collisionless fusion plasmas and that a kinetic thermal ion gap [20] is more appropriate than the ideal MHD BAAE gap to describe properties of low frequency spectra. Other kinetic effects such as trapped thermal particles could also be important for low frequency kinetic modes [21]. Therefore, a self-consistent gyrokinetic simulation treating both thermal and energetic particles on the same footing is required to resolve the outstanding controversy whether BAAE can be excited in the collisionless plasmas of fusion interest.

The outstanding controversy of BAAE existence in fusion plasmas is addressed in this letter by first-principles global simulations using gyrokinetic toroidal code (GTC) [22]. The current GTC simulations find that unstable BAAE and BAE can be simultaneously excited with similar radial mode width and comparable linear growth rates even though the damping rate of BAAE is much larger than BAE in the absence of energetic particles. This surprising result is attributed to non-perturbative effects of the energetic particles that modify ideal MHD mode polarizations and nonlocal geometry effects that invalidate radially local acoustic dispersion relation. In fact, simulation results show that unstable BAAE and BAE both have dominant Alfvenic polarizations for poloidal sidebands. On the other hand, the damped BAAE has dominant acoustic sidebands while the damped BAE has dominant Alfvenic sidebands. Direct calculations of wave-particle energy exchanges show that thermal ion Landau damping of the unstable BAAE is very weak (at a level similar to the BAE damping) due to the fact that the sidebands are dominated by Alfven polarizations and that the local acoustic dispersion relation is not valid for radially broad mode structure of the unstable BAAE. Following historical nomenclature, we continue to label this discrete low frequency mode as BAAE, but emphasize the importance of kinetic and nonlocal effects. These simulation results indicate that non-perturbative and radially nonlocal theory are required for properly describing the excitation of BAAE. Finally, GTC simulations with various tokamak sizes show that dominant mode changes from the BAAE in a larger tokamak to the BAE in a smaller tokamak due to the dependence of wave-particle resonance condition on the tokamak size.

Gyrokinetic simulations

GTC has been widely used to study Alfven eigenmodes [23–27] and other low frequency MHD modes in the tokamak [28, 29]. To elucidate BAAE excitation mechanism, we use GTC here to simulate a normal magnetic shear tokamak with a concentric circular cross-section, an on-axis magnetic field $B_0 = 1.91$ T, a major radius R_0 ranging from 2.6 m to 4.0 m, and a minor radius $a = 0.29R_0$. As shown in the panel (a) of figure 1, the safety factor profile is $q = 1.3721 + 0.5\psi - 0.1\psi^2$, where ψ is poloidal flux function normalized by the value at the separatrix. We use uniform profiles for electron density and temperatures of all species to minimize diamagnetic effects and coupling to kinetic ballooning mode and Alfvenic ion temperature gradient instability [10, 17, 21, 30].

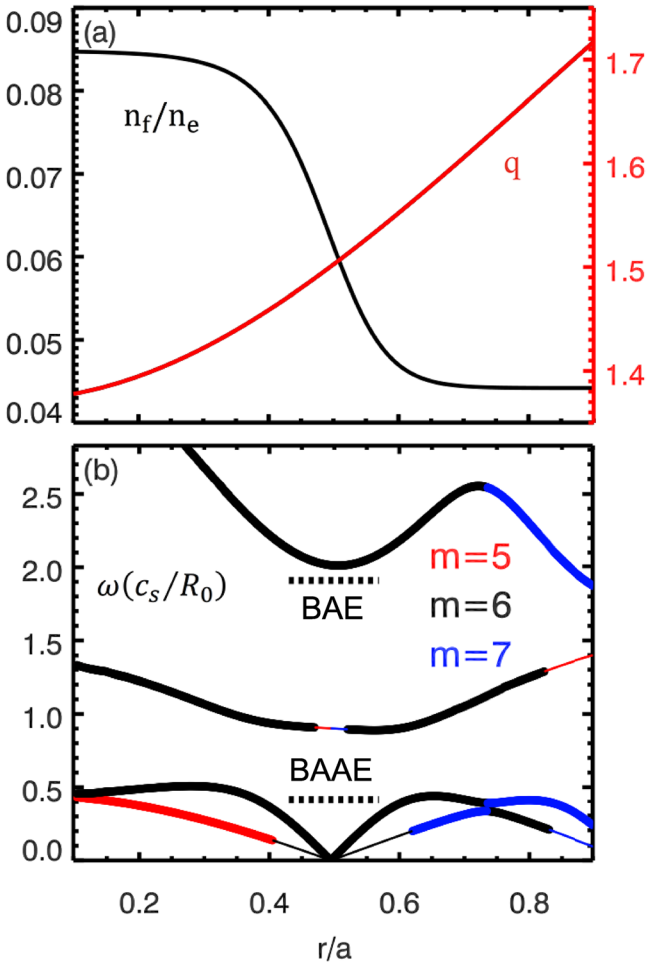

Figure 1. Panel (a): radial profiles of safety factor q and fast ion density n_f. Panel (b): low frequency continua of $n = 4$ mode in a tokamak calculated by ideal MHD ALCON eigenvalue code. Thick lines are Alfven branches and thin lines are acoustic branches. Horizontal dotted lines indicate BAE (upper gap) and BAAE (lower gap) frequencies and radial mode widths from gyrokinetic GTC simulations of energetic particle excitation.

The temperatures are $T_e = 2\,\text{keV}$, $T_i = 0.5T_e$, $T_f = 9T_e$ and the electron density is $n_e = 1.3 \times 10^{20}$ m^{-3} (electron beta $\beta_e = 2.87\%$). The fast ion density profile is $n_f = 0.085n_0\{1.0 + 0.24[\tanh(2.6 - 10\psi) - 1.0]\}$, and the thermal ion density is determined by the neutrality condition $n_f + n_i = n_e$. Both thermal and fast ions are proton and described by the gyrokinetic equations, while electrons are treated as a massless fluid [31]. Equilibrium plasma current and Coulomb collisions are neglected. A toroidal mode $n = 4$ is selected in linear simulation. Since BAAE has a very small parallel wavevector $k_{||} \sim 0$, we keep only poloidal harmonics $m \in [nq - 3, nq + 3]$, where $q = 1.5$ at the radial location with the steepest density gradients of fast ions. The spatial grids used in the simulation are $128 \times 512 \times 32$ in radial, poloidal, and parallel direction, respectively. The simulations use 20 particles per cell for both thermal and fast ions. Using similar parameters, our earlier GTC simulations show that [23] a low frequency unstable BAAE-like mode can be excited by realistic energetic particle density gradients in tokamaks with either normal or reversed magnetic

shear, even though the damped BAAE (in the absence of energetic particles) is heavily damped by the thermal ions.

The low frequency continuous spectra of the $n = 4$ mode in this tokamak equilibrium are calculated by the ideal MHD code ALCON [24] and plotted in the panel (b) of figure 1 for the frequency below toroidal Alfven frequency $\Omega_A = v_A/qR_0$, where Alfven speed is $v_A = B(4\pi n_i m_i)^{-1/2}$ and m_i is proton mass. The upper continuous spectrum is an Alfven continuum dominated by the principal poloidal harmonic $m = nq = 6$ (black thick line), i.e. $k_{||} \sim 0$ at the rational surface of $q = 1.5$ at $r = 0.5a$. The accumulation point (the minimal) frequency at the rational surface is the BAE frequency produced by geodesic acoustic compression $\Omega_{BAE} \sim (7T_i/2T_e + 2)^{1/2} c_s/R_0$, where sound speed is $c_s = (T_e/m_i)^{1/2}$. The middle continuous spectrum is an ion acoustic continuum created by the coupling of the Alfvenic principal poloidal harmonic $m = 6$ with the acoustic sidebands ($m = 5$ and 7), which has an accumulation point frequency produced by parallel compression $\Omega_{BAAE} \sim 2^{1/2} c_s/qR_0$. The lower continuous spectra include both Alfven and acoustic continua of the principal poloidal harmonic $m = 6$ with a zero-frequency at the mode rational surface. The lower gap between the acoustic continuum and the lower Alfven continuum is called BAAE gap, the upper gap between the acoustic continuum and the upper Alfven continuum is called BAE gap. A striking feature of the acoustic continuum is that the sidebands ($m = 5$ and 7) with the acoustic polarizations is only dominant in a very narrow region close to the rational surface. The principal harmonic ($m = 6$) with Alfvenic polarization is dominant over most of the radial domain. This feature has important implication on the excitation of discrete modes inside the BAAE gap, since the BAAE was expected by ideal MHD theory to have a radially localized mode structure with Alfvenic polarizations for the principal poloidal harmonic and acoustic polarizations for other poloidal sidebands. When kinetic effects of thermal plasmas are taken into account, a kinetic thermal ion gap appears in the low frequency spectra [20].

Dispersion relation and mode structure

GTC simulations of the $n = 4$ mode in a modest tokamak size $R_0 = 3.2$ m find that realistic density gradients of fast ions shown in the panel (a) of figure 1 can excite simultaneously discrete frequency modes of the BAAE in the lower gap and the BAE in the upper gap as shown in the panel (b) of figure 1. Both unstable modes ($k_\perp \rho_f = 0.093$) have similar growth rates ($\gamma_{BAAE} = 0.083 c_s/R_0$, $\gamma_{BAE} = 0.072 c_s/R_0$) even though BAAE Landau damping rate (normalized by its real frequency) is much larger than BAE damping rate. Both unstable modes have comparable radial mode widths, which are much broader than the radial domain of the acoustic sidebands in the acoustic continuum. The existence of such a radially extended, discrete frequency mode inside the BAAE gap has been verified by our earlier simulations using initial perturbation, antenna excitation, and energetic particle excitation for the ion temperature either smaller than or comparable to the electron temperature [23]. The BAAE excited by the antenna and energetic particles

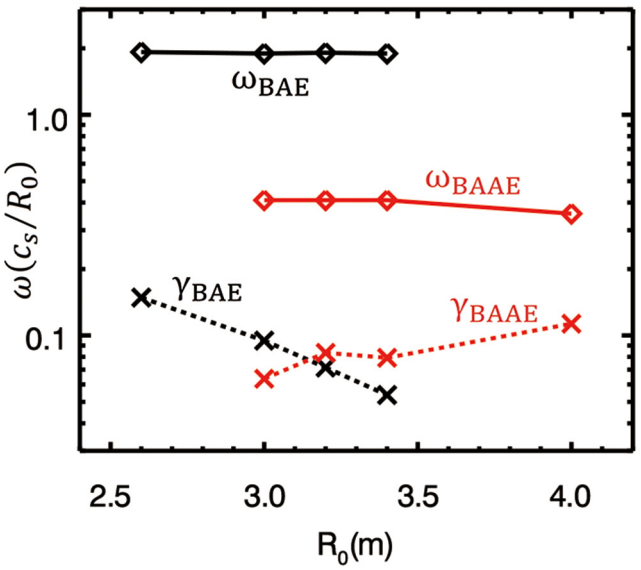

Figure 2. Frequencies (solid lines) and growth rate (dotted lines) of BAAE (red) and BAE (black) as a function of tokamak major radius R_0.

has similar frequency and radial location as that in the initial perturbation simulation, which demonstrates the existence of a damped BAAE even without kinetic effects of thermal ions or fast ions. This discrete frequency mode inside the BAAE gap has not been predicted by local or high-n theory, but has been observed from the ideal MHD global eigenvalue solver NOVA [11, 32]. Although the eigenmode structure is centered on the rational surface, the eigen-frequency is close to the maximum of the lower Alfven continuum, which is away from the rational surface. This may indicate that this eigenmode could be formed by nonlocal geometry effects, which have not been captured the by local or high-n ideal MHD theory that only predicts the Alfven-acoustic coupling on the mode rational surface and the associated existence of the BAAE frequency gap. Thus, the formulation of BAAE may require a radially nonlocal theory, e.g. by solving radial envelope equation in the ballooning mode theory taking into account kinetic effects of thermal plasmas [33].

By varying the tokamak major radius R_0 while keeping all dimensionless parameters unchanged, GTC simulations find that the BAAE dominates in a larger tokamak size (closer to ITER). For a smaller tokamak size (closer to existing tokamaks), the dominant mode is BAE (figure 2). This size dependence arises from the dependence of wave-particle resonance condition on the tokamak size [34]. Energetic particles drive BAAE through toroidal precessional resonances only, while BAE through all transit, drift-bounce, and precessional resonances.

The poloidal mode structures of electrostatic potentials $\delta\phi$ for BAAE and BAE are shown in figure 3 for various tokamak sizes. Both BAAE and BAE propagate in fast ion diamagnetic direction, i.e. clockwise direction on a poloidal plane when the toroidal magnetic field B_t points out of the poloidal plane. The BAAE mode structure in a large tokamak is characterized by a triangle shape pointing in the counter-clockwise direction, while the BAE in the clockwise direction. For the intermediate tokamak size, the mode structure

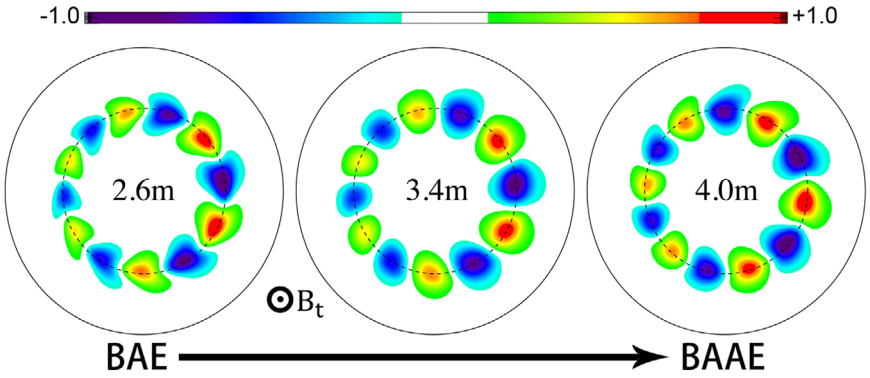

Figure 3. Poloidal contour plots of electrostatic potentials $\delta\phi$ of BAE and BAAE for various tokamak sizes R_0. The toroidal magnetic field B_t points out of the poloidal plane.

has no clear triangle shape due to the coexistence of BAE and BAAE, which have similar amplitudes at the time of the snapshot. If we run the simulation longer, the mode structure will be BAAE-like, because the BAAE growth rate is slightly larger but the initial amplitude is slightly smaller than BAE. The triangle shape of the BAAE electrostatic potential changes in reversed magnetic shear plasma, similar to that observed in tokamak experiments [23]. The physics of the difference in BAE and BAAE mode structures will be studied in future simulations.

Polarization and wave-particle energy exchanges

It is remarkable that both BAE and BAAE can be excited simultaneously with similar growth rates, even though the damping rate (normalized by the real frequency) of BAAE is much larger than BAE. To understand BAAE excitation mechanism, we examine mode polarizations and wave-particle energy exchanges for the $n = 4$ BAAE ($R_0 = 4.0$ m) and BAE ($R_0 = 2.6$ m) excited by fast ions. The radial profiles of the electrostatic potentials $\delta\phi$ are very similar for unstable BAE and BAAE as shown in panels (*a*) and (*e*) of figure 4. Both have a dominant principal poloidal harmonics $m = 6$ and two poloidal sidebands $m = 5$ and 7 peaking at the Alfven-acoustic coupling location. Panels (*b*) and (*f*) show very similar radial structures between BAAE and BAE for both the electrostatic parallel electric fields $E_{\parallel}^{\mathrm{ES}} = -\mathbf{b}_0 \cdot \nabla\delta\phi$ ($\mathbf{b}_0$ represents equilibrium magnetic field direction) and net parallel electric fields $E_{\parallel} = -\mathbf{b}_0 \cdot \nabla\delta\phi - \frac{1}{c}\frac{\partial \delta A_{\parallel}}{\partial t}$. The net parallel electric fields are much smaller than the electrostatic parallel electric fields for all poloidal harmonics, indicating that unstable BAAE and BAE are predominantly Alfvenic (thus small Landau damping by thermal ions).

The density gradients of fast ions are then gradually reduced until BAAE and BAE become stable in order to clarify the polarizations of damped BAAE and BAE, which are shown in panels (*c*) and (*g*), respectively. In contrast to the unstable BAAE, the damped BAAE have two poloidal sidebands ($m = 5$ and 7) that are predominantly electrostatic since the net parallel electric fields shown in panel (*c*) are comparable to the electrostatic parallel electric fields, i.e. acoustic polarizations. On the other hand, the damped BAE mode is still mostly Alfvenic as shown in panel (*g*). The fact that the poloidal sidebands of the damped BAAE are primarily acoustic highlights the significance of the coupling between Alfven and acoustic continua. However, the polarizations are very different between the unstable and damped BAAE, indicating the strong non-perturbative effects of the fast ions. Furthermore, when the BAAE changes from unstable to damped modes as density gradients of the fast ions are gradually reduced, the BAAE frequency gradually increases, which brings the dispersion relation closer to the ion acoustic wave and thereby increase the acoustic polarizations and associated Landau damping by thermal ions. These results demonstrate the strong non-perturbative effects of the fast ions on the BAAE mode structure and polarization, and ultimately the mode excitation.

Since Alfvenic polarization dominates all poloidal harmonics of unstable BAAE, the Landau damping by thermal ions is expected to be small. This is verified by direct calculations of energy exchanges between the ions and the waves as shown in panels (*d*) and (*h*) for the unstable BAAE and BAE, respectively. The rate of changes of wave energy δW can be calculated from the power of work done on the particles by the waves:

$$\frac{\partial \delta W}{\partial t} = \left\langle -Z\mathbf{v}_{\perp} \cdot \mathbf{E}_{\perp} - Zv_{\parallel}E_{\parallel} \right\rangle .$$

Here, $v_{\parallel}$ is linear guiding center parallel velocity, $\mathbf{v}_{\perp}$ is guiding center curvature and grad-B perpendicular drifts, $\mathbf{E}_{\perp} = -\nabla_{\perp}\delta\phi$ is perpendicular electrostatic field, Z is particle charge, and $\langle \cdots \rangle$ represents gyro-average and summation over distribution function and flux-surfaces. As shown in panels (*d*) and (*h*) for parallel and perpendicular energy exchanges, both BAAE and BAE are excited mostly by perpendicular energy transfer from fast ions to waves. The energy transfer occurs through toroidal precessional resonances of the fast ions with BAAE, and transit, drift-bounce, precessional resonances with BAE [34]. The parallel energy transfer from fast ions is very small for both BAE and BAAE. On the other hand, the damping by thermal ions is somewhat different between unstable BAAE and BAE. The BAAE damping is through both parallel and perpendicular energy transfers to thermal ions, while BAE damping is dominated by perpendicular energy transfer to thermal ions. This is due to different real frequencies: the BAAE has a lower frequency and thus a phase velocity closer

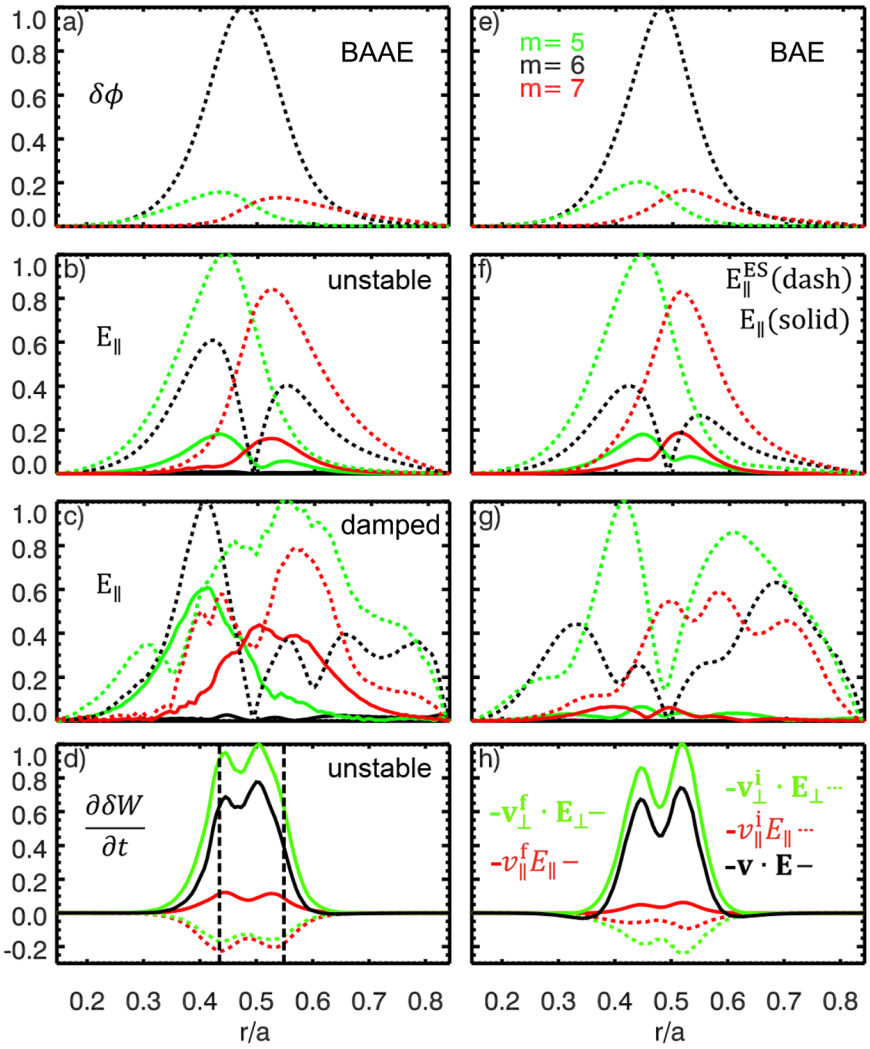

Figure 4. Radial profiles of BAAE (left column) and BAE (right column) electrostatic potentials $\delta\phi$ ((*a*) and (*e*)), electrostatic (dotted) and net (solid) parallel electric fields $E_\parallel$ of unstable modes ((*b*) and (*f*)) and damped modes ((*c*) and (*g*)), and rate of change of wave energy $\frac{\partial \delta W}{\partial t}$ for unstable modes ((*d*) and (*h*)) due to energy transfer from energetic (solid) and thermal (dotted) ions.

to the parallel velocity of thermal ions. The Landau damping of BAAE by thermal ions peaks at the radial location of the Alfven-acoustic coupling, i.e. $k_\parallel v_A = \omega_{BAAE} \sim c_s/qR_0$, as marked by the two vertical dashed lines in panel (*d*).

The Landau damping rate by thermal ions can be calculated using the power in panels (*d*) and (*h*). We find that the Landau damping rate of unstable BAAE of panel (*b*) is $\gamma_{D\_unstable} = -0.075 c_s/R_0$, which is similar to the damping rate of BAE of panel (*f*) ($\gamma_{D\_unstable} = -0.098 c_s/R_0$). On the other hand, the Landau damping rate of damped BAAE without energetic particles is $\gamma_{D\_damped} = -0.18 c_s/R_0$ [23, 34], which is much larger than the damping rate of unstable BAAE of panel (*b*) or damped BAE (in the absence of energetic particles) [34] ($\gamma_{D\_damped} = -0.034 c_s/R_0$). The reduction of the BAAE damping rate in the presence of fast ions is clearly due to the change of the sideband polarizations from acoustic to Alfvenic. The damping rate of the unstable BAE is larger than the damped BAE due to the larger parallel electric field in the unstable BAE because of the non-perturbative effects of energetic particles. Therefore, the non-perturbative and nonlocal theory is required to properly describe the excitation of BAAE (and, to a lesser extent, BAE) by fast ions in tokamaks.

In summary, global gyrokinetic simulations find that realistic density gradients of energetic particles can simultaneously excite low frequency Alfven eigenmodes in toroidal geometry, BAAE and BAE, with similar radial mode widths and comparable linear growth rates even though damping rate of BAAE is much larger than BAE in the absence of energetic particles. This surprising result is attributed to non-perturbative effects of energetic particles that modify ideal BAAE mode polarizations and nonlocal geometry effects that invalidate radially local dispersion relation.

Acknowledgments

This work was supported by the US Department of Energy (DOE) SciDAC GSEP center and by China National Magnetic Confinement Fusion Science Program (Grants No. 2013GB111000) and China Scholarship Council, and used resources of the Oak Ridge Leadership Computing

Facility at Oak Ridge National Laboratory (DOE Contract No. DE-AC05-00OR22725), and the National Energy Research Scientific Computing Center (DOE Contract No. DE-AC02-05CH11231).

ORCID

Wenlu Zhang https://orcid.org/0000-0002-7136-2119

References

[1] Chen L. and Zonca F. 2016 *Rev. Mod. Phys.* **88** 015008
[2] Giacalone J. and Jokipii J.R. 1999 *Astrophys. J.* **520** 204
[3] Gorelenkov N.N., Berk H.L., Fredrickson E., Sharapov S.E. and JET EFDA Contributors 2007 *Phys. Lett.* A **370** 70
[4] Heidbrink W.W., Strait E.J., Chu M.S. and Turnbull A.D. 1993 *Phys. Rev. Lett.* **71** 855
[5] Sabot R. *et al* 2009 *Nucl. Fusion* **49** 085033
[6] Chen W. *et al* 2010 *Phys. Rev. Lett.* **105** 185004
[7] Elfimov A.G. *et al* 2011 *Plasma Phys. Control. Fusion* **53** 025006
[8] Nazikian R. *et al* 2006 *Phys. Rev. Lett.* **96** 105006
[9] Winsor N., Johnson J.L. and Dawson J.J. 1968 *Phys. Fluids* **11** 2448
[10] Gorelenkov N.N., Van Zeeland M.A., Berk H.L., Crocker N.A., Darrow D., Fredrickson E., Fu G.Y., Heidbrink W.W., Menard J. and Nazikian R. 2009 *Phys. Plasmas* **16** 056107
[11] Gorelenkov N.N. *et al* 2007 *Plasma Phys. Control. Fusion* **49** B371
[12] Darrow D.S., Fredrickson E.D., Gorelenkov N.N., Roquemore A.L. and Shinohara K. 2008 *Nucl. Fusion* **48** 084004
[13] Curran D., Lauber P., Mc Carthy P.J., da Graca S., Igochine V. and the ASDEX Upgrade Team 2012 *Plasma Phys. Control. Fusion* **54** 055001
[14] Isobe M., Ogawa K., Shimizu A., Osakabe M., Kubo S., Toi K. and the LHD Experiment Group 2015 *Plasma Sci. Technol.* **17** 276
[15] Deng C.B. *et al* 2009 *Phys. Rev. Lett.* **103** 025003
[16] Haskey S.R., Blackwell1 B.D., Nührenberg C., Könies A., Bertram J., Michael C., Hole M.J. and Howard J. 2015 *Plasma Phys. Control. Fusion* **57** 095011
[17] Lauber P. 2013 *Phys. Rep.* **533** 33
[18] Fisch N.J. and Rax J.M. 1992 *Phys. Rev. Lett.* **69** 612
[19] Zonca F., Biancalani A., Chavdarovski I., Chen L., Di Troia C. and Wang X. 2010 *J. Phys.: Conf. Ser.* **260** 012022
[20] Chen L. and Zonca F. 2007 *Nucl. Fusion* **47** S727
[21] Chavdarovski I. and Zonca F. 2014 *Phys. Plasmas* **21** 052506
[22] Lin Z., Hahm T.S., Lee W.W., Tang W.M. and White R.B. 1998 *Science* **281** 1835
[23] Zhang H.S., Liu Y.Q., Lin Z. and Zhang W.L. 2016 *Phys. Plasmas* **23** 042510
[24] Deng W., Lin Z., Holod I., Wang Z., Xiao Y. and Zhang H. 2012 *Nucl. Fusion* **52** 043006
[25] Zhang H.S., Lin Z. and Holod I. 2012 *Phys. Rev. Lett.* **109** 025001
[26] Wang Z.X., Lin Z., Holod I., Heidbrink W.W., Tobias B., Van Zeeland M. and Austin M.E. 2013 *Phys. Rev. Lett.* **111** 145003
[27] Cheng J.Y., Zhang W.L., Lin Z., Holod I., Li D., Chen Y. and Cao J.T. 2016 *Phys. Plasmas* **23** 052504
[28] McClenaghan J., Lin Z., Holod I., Deng W. and Wang Z. 2014 *Phys. Plasmas* **21** 122519
[29] Liu D.J., Zhang W.L., McClenaghan J., Wang J.Q. and Lin Z. 2014 *Phys. Plasmas* **21** 122520
[30] Zonca F., Chen L., Dong J.Q. and Santoro R.A. 1999 *Phys. Plasmas* **6** 1917
[31] Holod I., Zhang W.L., Xiao Y. and Lin Z. 2009 *Phys. Plasmas* **16** 122307
[32] Gorelenkov N.N., Pinches S.D. and Toi K. 2014 *Nucl. Fusion* **54** 125001
[33] Chen L. and Zonca F. 2017 *Phys. Plasmas* **24** accepted
[34] Liu Y.Q., Lin Z., Zhang H.S. and Zhang W.L. 2017 Linear wave-particle interactions of low frequency Alfven eigenmodes in tokamak in preparation